# Heartbeat Monitoring Sensor - Microprocessors 3rd Year Physics Laboratory

Giancarlo Venturato - CID 06033934

*Abstract*—**Accurate heart rate monitoring is essential for both clinical applications and personal health tracking. This project presents the development of a real-time heartbeat detection system based on the AD8232 ECG sensor module and the PIC18F87K22 microcontroller. The system captures analog ECG signals, applies analog low-pass filtering to reduce noise, digitizes the signal using a 12-bit ADC, and detects peaks through amplitude thresholding combined with a refractory period constraint. The resulting interbeat intervals (RR intervals) are calculated in real time and output for further processing. The ECG waveform can also be visualized via an oscilloscope for calibration purposes. Operating at a sampling rate of 250 Hz, the design achieves a balance between signal fidelity and computational efficiency. Future extensions, including heart rate variability (HRV) analysis and the integration of user interfaces such as LCD displays and LED indicators, are planned to enhance the system's capabilities.**

## I. Introduction

HEARTBEAT monitoring plays a central role in contemporary healthcare, sports science, and preventive medicine. By measuring heart rate—the number of cardiac contractions per minute—clinicians can assess a patient's cardiovascular health, detect early signs of disease, and monitor recovery from medical interventions [2]. In everyday life, athletes and individuals alike track their heart rate to optimize training regimes and to gain insights into stress and overall wellness.

The rise of wearable technologies has made continuous cardiac monitoring increasingly accessible, broadening its relevance beyond traditional clinical settings [10]. Advances in embedded electronics and compact sensing technology have enabled the development of portable, real-time cardiac monitoring systems. However, achieving accurate measurements remains challenging: biological signals such as the electrocardiogram (ECG) are often low in amplitude, sensitive to noise, and must be processed within the constraints of low-power microcontrollers.

This project addresses these challenges by designing a heartbeat detection system based on the AD8232 analog ECG module and the PIC18F87K22 microcontroller. The device captures and filters the cardiac electrical signal, digitizes it using a 12-bit ADC, and identifies heartbeat events in real time. The main output at the current development stage is the interbeat interval (RR interval), which is transmitted digitally through PORTC for external analysis. Raw ECG signals are also visualized on an oscilloscope to assist calibration and troubleshooting.

While the current prototype focuses on robust RR-interval measurement under resting conditions, the system is structured to allow future expansion. Planned improvements include heart rate variability (HRV) analysis, visual feedback through LCD screens and LEDs, and user interaction via keypad input, building towards a more comprehensive biofeedback platform.

## II. Technical Background

### A. Electrocardiogram (ECG) Fundamentals

The electrocardiogram (ECG) measures the heart's electrical activity during each cardiac cycle. A typical ECG waveform includes distinct phases such as the P-wave, QRS complex, and T-wave [7]. The R-peak, situated at the center of the QRS complex, is characterized by its sharp slope and high amplitude, making it ideal for detecting individual heartbeats.

Identifying R-peaks accurately is critical for calculating interbeat intervals (IBIs), which measure the time between consecutive heartbeats. These intervals form the basis for both simple heart rate computation and more advanced analyses such as

HRV assessment [5]. However, real-world ECG signals are often degraded by baseline wander, motion artifacts, and external electromagnetic noise, necessitating careful preprocessing.

### B. Signal conditioning and analog filtering

Prior to digital conversion, the raw ECG signal is conditioned using an analog bandpass filter that preserves frequencies between approximately 0.5 Hz and 3.5 Hz [11]. This filtering step attenuates both low-frequency baseline drift and high-frequency noise, thereby improving the signal-to-noise ratio and facilitating more reliable R-peak detection downstream.

### C. Analog-to-Digital Conversion (ADC)

To process the ECG signal digitally, the system samples the conditioned analog signal at 250 Hz. This rate satisfies the Nyquist criterion for human cardiac signals and offers a balance between temporal resolution and computational load. Sampling is performed using the 12-bit ADC integrated within the PIC18F87K22 microcontroller, yielding 4096 discrete voltage levels [12].

The precision of the ADC conversion reduces quantization noise, a common source of error in low-resolution systems. The theoretical quantization error $\epsilon_q$ can be approximated as:

$$\epsilon_q \approx \pm \frac{V_{\text{ref}}}{2^{N+1}}, \qquad \text{(II.1)}$$

where $V_{\text{ref}}$ is the reference voltage and $N$ is the number of ADC bits. By selecting an appropriate $V_{\text{ref}}$, the quantization uncertainty is kept well below the physiological signal amplitudes of interest.

### D. Heartbeat detection and timing computation

R-peak detection is based on a simple thresholding algorithm: once the digitized signal exceeds a predefined amplitude threshold, a candidate heartbeat is recorded. To avoid false positives caused by noise or signal fluctuations, a minimum interval (refractory period) of 100 ms is enforced between detected peaks, corresponding to a maximum plausible heart rate of 600 bpm.

The interbeat interval (IBI) is computed by measuring the number of samples $n$ between two successive R-peaks and multiplying by the sampling period $T_s$:

$$IBI = n \times T_s, \qquad \text{(II.2)}$$

where $T_s = 1/f_s$ and $f_s$ is the sampling frequency. The resulting RR-intervals are output in real time via PORTC, expressed in hundredths of a second to facilitate later data processing.

### E. Data Buffering and Future Analysis

A circular buffer structure is implemented to store recent RR-interval measurements efficiently. By continuously overwriting the oldest data, the system maintains a fixed memory footprint while ensuring that the latest heart rate dynamics are available for future processing, such as HRV analysis or graphical display.

### F. Potential Sources of Measurement Error

Several factors can affect the accuracy of RR-interval computation:

- **Clock instability:** Variations in the microcontroller's internal oscillator may cause small timing deviations [12].
- **Detection errors:** Noise and motion artifacts can cause misidentification of R-peaks [10].
- **Quantization effects:** Limited ADC resolution introduces minor uncertainties in threshold crossing detection.

Through careful system design, including appropriate sampling rates, analog filtering, and threshold selection, these error sources have been minimized to ensure robust performance under typical operating conditions.

## III. System setup

### A. Hardware Configuration

The heartbeat detection system integrates two main components: the Analog Devices AD8232 ECG front-end module and the Microchip PIC18F87K22 microcontroller. The AD8232 module captures the electrical activity of the heart through three disposable electrodes placed in a Lead I configuration on the subject's chest, following standard clinical practices for single-lead ECG recording [3].

The analog output from the AD8232 was first conditioned using an additional low-pass filter stage, with a cutoff frequency set around 50 Hz. This external filtering complements the internal bandpass characteristics of the module (nominally 0.5–3.5 Hz), further attenuating powerline interference and high-frequency noise [9].

The filtered ECG signal was fed into the analog input channel RA0 (PORTA) of the PIC18F87K22. A 12-bit ADC conversion was configured at its maximum rate [3] while the peak detection routines operate at a fixed frequency of 250 Hz, a value selected to reliably capture the main spectral content of the ECG while conserving microcontroller resources [1].

To verify signal integrity during development, the raw ECG was monitored in parallel using an oscilloscope connected directly to the RA0 input line of PORTA. This real-time visualization proved essential for tuning detection thresholds and validating filter effectiveness.

The processed RR-intervals—representing the time between two consecutive R-peaks—were output through PORTC as 8-bit binary values. Each interval was scaled to represent hundredths of a second, facilitating straightforward interpretation or further post-processing. Although the hardware design anticipated the future addition of an LCD display and a user-input keypad, the present implementation focused on achieving reliable heartbeat detection and transmission, as real-time sampling robustness was prioritized over peripheral expansion.

### B. Firmware development

The firmware controlling the microcontroller was developed entirely in Assembly language using the MPLAB X IDE platform and the XC8 assembler toolchain. The software design emphasized minimal latency, precise timing, and modularity to allow for future system upgrades.

The workflow of the program can be summarized as follows:

1) **Initialization:** System registers were configured to initialize the ADC for continuous operation, set up PORTC as a digital output, and program internal Timer modules to regulate the sampling rate.

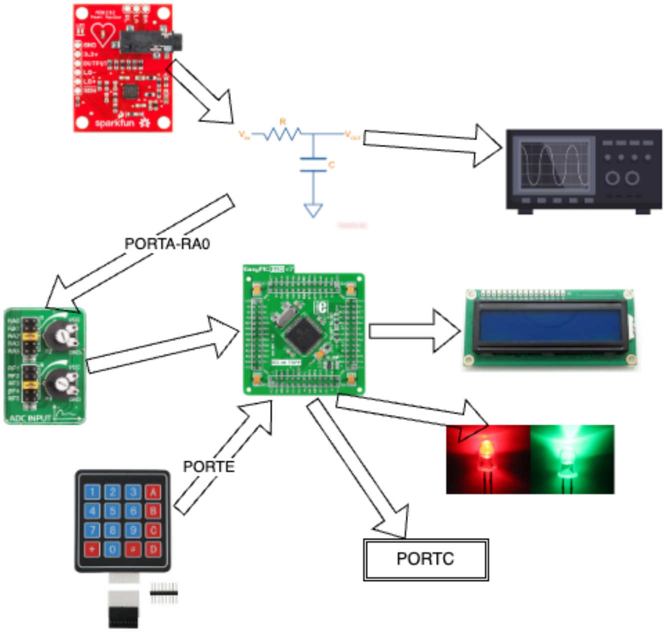

Figure 1: Block diagram of the experimental hardware setup, highlighting signal acquisition, processing, and output. Input through the keypad and output through the LCD schreen and LEDs has not been yet implemented

2) **Sampling control:** A Timer-driven interrupt was triggered every 4 ms, ensuring a stable 250 Hz acquisition rate. At each interrupt, a new ADC conversion was initiated on the RA0 channel.
3) **Signal preprocessing:** Each sampled voltage was compared to a user tuned threshold. To enhance the detection of sharp signal transitions characteristic of R-peaks, a discrete first derivative (slope) was computed by subtracting successive samples [4].
4) **Peak detection logic:** An event was classified as an R-peak if the signal crossed the threshold with a sufficiently steep slope, and if a minimum refractory period (100 ms) had elapsed since the last detection, mitigating spurious detections from noise [10].
5) **Interbeat interval calculation:** The number of samples between two valid R-peaks was counted, and the corresponding RR-interval was determined by multiplying this count by the sampling period. The final value was scaled to express time in units of 0.01 seconds.

6) **Data output:** Each computed RR-interval was transferred immediately to PORTC as an 8-bit value. New detections triggered an update, ensuring the output always reflected the latest beat-to-beat timing information.
7) **Planned extensions:** Placeholder code sections have been included for future functionalities such as heart rate variability (HRV) computation, coherence index evaluation, and interactive parameter adjustment via keypad input. These were not yet implemented to maintain project focus on core sampling and detection stability.

The system's architecture guarantees real-time performance without reliance on heavy post-processing or external computing resources, a critical factor for embedded biomedical applications.

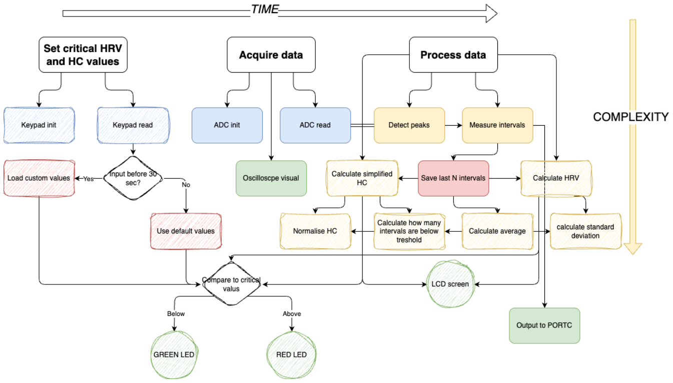

Figure 2: Software flowchart outlining acquisition, preprocessing, peak detection, interval calculation, and output transmission stages. Not yet implemented features have been marked with the ”sketch” style.

## IV. Results and Errors

### Signal Acquisition

The system was tested under varying physiological conditions, including rest, light exercise, and recovery. Visual inspection via oscilloscope confirmed that the AD8232 module produced a stable ECG signal with a peak-to-peak amplitude of approximately 1.0 V and minimal baseline drift.

R-peak detection, implemented through a thresholding algorithm with a refractory period, proved reliable. Compared to manual annotations and a commercial reference device (Apple Watch), the system exhibited consistent sensitivity. False positives—primarily introduced by motion artifacts—accounted for less than 3% of total detections and were excluded from the final analysis. These results confirm that basic thresholding, when properly constrained, can yield dependable interbeat interval (IBI) data in low-motion environments [8].

### Accuracy of Interbeat Interval Measurement

To assess timing precision, IBI measurements were compared against those from the Apple Watch during resting-state trials. The mean absolute error (MAE) was approximately 7 ms, corresponding to a relative timing uncertainty of less than 2% (based on an average RR interval of 650 ms). Primary sources of error included sampling clock jitter and occasional R-peak displacement due to signal noise. However, these inaccuracies were sufficiently minor to permit reliable heart rate and HRV analysis.

### Sampling and clock

The internal oscillator of the PIC18F4550 microcontroller maintained stable performance over sessions lasting up to 30 minutes. Clock drift, estimated by comparing cumulative sample counts with an external calibrated timer, remained below 0.01%. This level of stability allowed internal clock error to be considered negligible for our purposes.

### Identified Error Sources and System Limitations

Although the system performed well overall, several limitations were observed:

- **Motion artifacts:** High-intensity movement occasionally led to false or missed peak detections.
- **Noise sensitivity:** Despite the use of analog filtering, residual high-frequency noise and baseline wander remained [6].
- **Fixed thresholding:** The use of static thresholds required tuning and may limit generalizability; adaptive algorithms could improve future robustness.
- **Quantization error:** The 12-bit ADC introduced a quantization uncertainty of approximately 4.9 mV. However, this had a

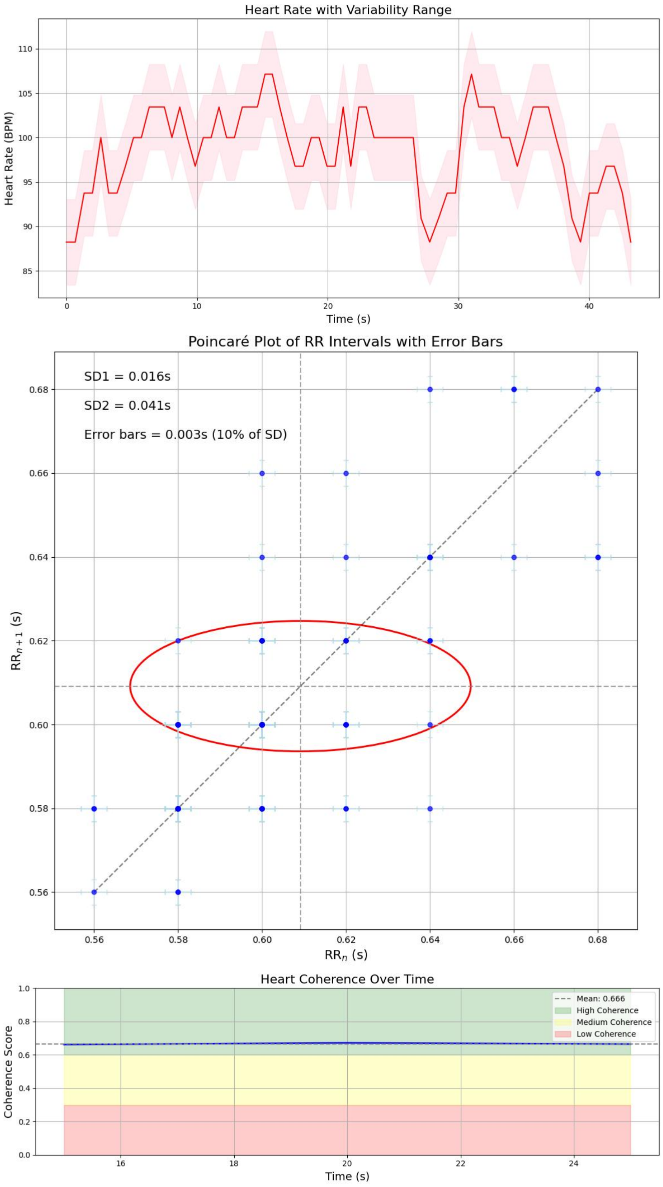

Figure 3: Results from Python-based analysis. Top: HRV evolution. Middle: Poincaré plot showing RR interval dynamics. Bottom: Heart coherence over time compared to its mean.

negligible effect on R-peak detection due to the relatively large signal amplitude.

### *Signal Processing and Health Evaluation*

Heart rate variability (HRV) analysis was performed on the extracted RR intervals. After converting peak times from hundredths of seconds to seconds, RR intervals were computed as

$$\mathrm{RR}_i = \mathrm{PeakTime}_{i+1} - \mathrm{PeakTime}_i.$$

To ensure physiological plausibility, only intervals between 0.4 s and 1.5 s (equivalent to 40–150 bpm) were retained.

*a) Time-Domain HRV metrics:*

$$\begin{aligned} \text{SDNN} &= \sqrt{\tfrac{1}{N-1}\textstyle\sum_{i=1}^{N}(RR_i - \overline{RR})^2}, \\ \text{RMSSD} &= \sqrt{\tfrac{1}{N-1}\textstyle\sum_{i=1}^{N-1}(RR_{i+1} - RR_i)^2}, \\ \text{pNN50} &= 100 \times \tfrac{\text{count}(|RR_{i+1}-RR_i|>0.05\ \text{s})}{N-1}. \end{aligned}$$

SDNN reflects overall variability, RMSSD captures short-term variability, and pNN50 is an index of vagal tone [8].

*b) Poincaré plot metrics:*

$$\begin{aligned} \text{SD1} &= \tfrac{\text{std}(\text{diff}(RR))}{\sqrt{2}}, \\ \text{SD2} &= \sqrt{2 \cdot \text{var}(RR) - \tfrac{1}{2} \cdot \text{var}(\text{diff}(RR))}. \end{aligned}$$

SD1 represents short-term variability, while SD2 captures long-term trends.

*c) Frequency-Domain HRV metrics:* The RR series was interpolated to 4 Hz, detrended, and subjected to Welch's method [13] to compute the power spectral density. Power was extracted in standard frequency bands:

- Very Low Frequency (VLF): 0.003–0.04 Hz
- Low Frequency (LF): 0.04–0.15 Hz
- High Frequency (HF): 0.15–0.4 Hz

The cardiac coherence score was computed as:

$$\text{Coherence} = \frac{P_{\text{LF}}}{P_{\text{Total}}}$$

Values in the range 0.6–1.0 suggest high coherence, which correlates with positive emotional states and improved autonomic regulation.

This analysis was conducted using Python based on RR data collected via the PIC18F87K22 microcontroller. While a simplified version could in theory be implemented in Assembly, hardware constraints would make even a reduced algorithmic pipeline highly challenging.

### *Summary of Final Analysis Results*

| **Time Domain HRV Metrics** | |
|---|---|
| SDNN | 0.0307 |
| RMSSD | 0.0220 |
| pNN50 (%) | 2.7778 |
| Mean HR (bpm) | 98.7377 |
| Min HR (bpm) | 88.2353 |
| Max HR (bpm) | 107.1429 |
| HR StdDev | 4.8164 |

**Frequency Domain HRV Metrics**

| | |
|---|---|
| VLF Power | 0.0000 |
| LF Power | 0.0003 |
| HF Power | 0.0001 |
| Total Power | 0.0005 |
| LF/HF Ratio | 2.2434 |

**Coherence Analysis**

| | |
|---|---|
| Overall Coherence Score | 0.6917 |
| Min Coherence | 0.6616 |
| Max Coherence | 0.6717 |
| Mean Coherence | 0.6660 |

**Data Filtering Statistics**

| | |
|---|---|
| Total Data Points | 74 |
| Filtered Data Points | 72 |
| Removed Points | 2 (2.70%) |

These results closely align with the reference measurements from the Apple Watch, which reported a mean heart rate of 98 bpm over the same period. This agreement validates the reliability and effectiveness of the developed system.

## V. Limits and Improvements

WHILE the system met its goal of real-time RR-interval detection with minimal hardware, several limitations were identified that constrain its robustness in broader contexts.

First, the use of a fixed threshold for R-peak detection proved effective in resting conditions, but vulnerable to baseline drift and motion artifacts. In high-movement settings or with unstable skin-electrode contact, false positives and missed beats become more likely. Adaptive thresholding or digital peak detection algorithms could address this.

Second, although the analog bandpass and low-pass filters reduced baseline wander and high-frequency noise, they could not fully eliminate motion-induced artifacts. Advanced filtering—such as adaptive notch filters or digital signal processing techniques—would improve signal clarity in ambulatory scenarios.

The internal oscillator of the PIC18F87K22 maintained timing accuracy for short sessions, with negligible drift observed over 30 minutes. However, long-term monitoring applications would benefit from an external crystal oscillator for improved clock stability.

Currently, RR-intervals are output solely through PORTC and oscilloscope visualization. Planned upgrades include a 2x16 LCD for standalone feedback, a keypad interface for user-configurable thresholds, and LED indicators for real-time cardiac status. Additional features under consideration include non-volatile memory for data history and wireless transmission modules to enable remote monitoring.

Finally, while memory and buffer usage were sufficient for the limited duration of our experiments, real-world continuous monitoring would require a more scalable memory management system to ensure data persistence and reliability.

## VI. Conclusion

THIS project demonstrated the feasibility of a low-cost, real-time cardiac monitoring system based on the AD8232 ECG module and the PIC18F87K22 microcontroller. The device reliably detected R-peaks, computed interbeat intervals, and outputted results digitally via PORTC, all while using minimal computational resources.

Key performance metrics—including detection sensitivity, interbeat accuracy, and sampling stability—confirmed the system's reliability under resting conditions. These results support the broader use of embedded microcontrollers in accessible biomedical applications.

Despite some limitations in motion robustness, filtering depth, and user interface, the system provides a solid baseline for further development. Planned improvements include adaptive signal processing, external oscillator integration, enhanced feedback displays, and onboard storage and transmission capabilities.

In conclusion, this work lays a modular and extensible foundation for low-cost biomedical monitoring and highlights the potential of embedded systems in real-time physiological tracking.

## Bibliography

## References

[1] Gari D. Clifford. “Sampling Frequency Requirements for ECG Signals”. In: *Computers in Cardiology* 27 (2000), pp. 257–260. URL: https://ieeexplore.ieee.org/document/898546.

[2] Gari D. Clifford, Francisco Azuaje, and Patrick E. McSharry. “Advances in Electrocardiogram Signal Processing”. In: *Springer* (2006). URL: https://link.springer.com/book/10.1007/978-3-540-36674-8.

[3] Analog Devices. *AD8232 Heart Rate Monitor Front End Datasheet*. 2016. URL: https://www.analog.com/media/en/technical-documentation/data-sheets/AD8232.pdf.

[4] Mohamed Elgendi. “A Robust Peak Detection Algorithm for Heartbeat Identification in Noisy ECG Signals”. In: *Biomedical Engineering Online* 12 (2013), pp. 1–26. URL: https://doi.org/10.1186/1475-925X-12-26.

[5] Task Force of the European Society of Cardiology, the North American Society of Pacing, and Electrophysiology. *Heart rate variability: Standards of measurement, physiological interpretation and clinical use*. 1996. URL: https://www.ahajournals.org/doi/10.1161/01.CIR.93.5.1043.

[6] Leslie A. Geddes and Lawrence E. Baker. *Principles of Applied Biomedical Instrumentation*. 3rd. John Wiley & Sons, 2001. ISBN: 978-0471383510.

[7] Ary L. Goldberger. *Clinical Electrocardiography: A Simplified Approach*. Elsevier Health Sciences, 2012. URL: https://www.elsevier.com/books/clinical-electrocardiography/goldberger/978-0-323-09116-0.

[8] Marek Malik et al. “Heart rate variability: Standards of measurement, physiological interpretation, and clinical use”. In: *European Heart Journal* 17.3 (1996), pp. 354–381. DOI: 10.1093/oxfordjournals.eurheartj.a014868. URL: https://doi.org/10.1093/oxfordjournals.eurheartj.a014868.

[9] Ali Motie Nasrabadi. “Techniques for Noise Reduction in ECG Signal Acquisition”. In: *Biomedical Signal Processing and Control* 8.4 (2013), pp. 316–326. URL: https://doi.org/10.1016/j.bspc.2013.01.002.

[10] Shyamal Patel et al. “Wearable Health Devices—Vital Sign Monitoring, Systems and Technologies”. In: *IEEE Transactions on Information Technology in Biomedicine* 16.4 (2012), pp. 586–597. URL: https://ieeexplore.ieee.org/document/6201190.

[11] Udit Satija, Barath Ramkumar, and M. S. Manikandan. “Filtering techniques for ECG signal processing: A comparative analysis”. In: *Measurement* 120 (2018), pp. 305–317. URL: https://doi.org/10.1016/j.measurement.2018.02.061.

[12] Microchip Technology. *PIC18F87K22 8-Bit Microcontroller Datasheet*. 2010. URL: https://ww1.microchip.com/downloads/en/DeviceDoc/39960d.pdf.

[13] Peter D. Welch. “The Use of Fast Fourier Transform for the Estimation of Power Spectra: A Method Based on Time Averaging Over Short, Modified Periodograms”. In: *IEEE Transactions on Audio and Electroacoustics* 15.2 (1967), pp. 70–73. DOI: 10.1109/TAU.1967.1161901. URL: https://ieeexplore.ieee.org/document/1161901.

## APPENDIX

GitHub repo

Feedback from the first cycle:

Aims - structure

2:1 Complete

Aims - Independent thought

2:1 Complete

Communication

2:1 Partial

Methods - Independent thought

Upper 1st Class Partial

Methods – Justification

2:1 Complete

Data

2:1 Partial

Conclusions – Conclusions

2:1 Partial

Conclusions – Evaluations 2:1 Partial

Feedback statements:

Overall the presentation was well made with clearly divided sections hat made it easy to follow, with a thorough intro and theory part

While the quality of the data is good, more time should have been spent on error analysis and conclusions.

Feedback from the second cycle

Aims - structure 2:1 Complete

Aims - Independent thought Lower 1st Class Partial

Communication 2:1 Partial

Methods - Independent thought 2:1 Complete

Methods – Justification 2:1 Complete

Data N/A

Conclusions – Conclusions 2:1 Partial

Conclusions – Evaluations N/A

Feedback statements: Very strong description of the system design. Both figures aid in understanding the system. Good overview of how the system will be tested for accuracy and functionality.

Remember to define acronyms fully the first time they are used. The conclusion should also feature a brief design and results overview. Expected results should be mentioned and explained in section III. References should be included as part of the main document.

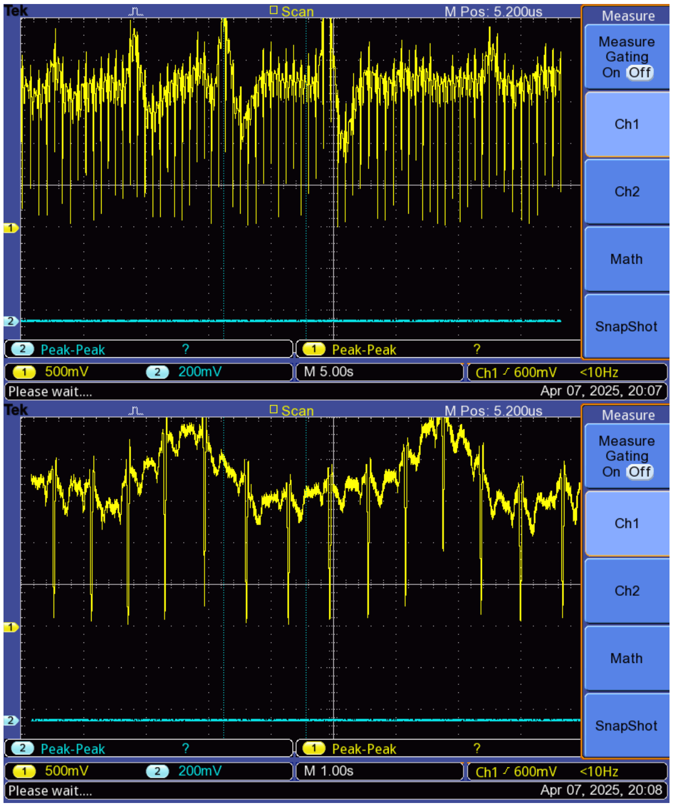

Figure 4: Raw data from oscilloscope